Discrimination of Single-Nucleotide Alterations by G-Specific Fluorescence Quenching

Chikara Dohno[b, c] and Isao Saito*[a, c]

A new strategy for the detection of single-base alterations through fluorescence quenching by guanine (G) is described. We have devised a novel base-discriminating fluorescent (BDF) nucleoside, 4′PyT, that contains a pyrenecarboxamide fluorophore at the thymidine sugar's C4′-position. 4′PyT-containing oligodeoxynucleotides only exhibited enhanced fluorescence in response to the presence of a complementary adenine base. In contrast, the fluorescence of mismatched duplexes containing 4′PyT/N base pairs (N = C, G, or T) was considerably weaker. This highly A-selective fluorescence was a product of guanine-specific quenching efficiency; when the complementary base to 4′PyT was a mismatch, the pyrenecarboxamide fluorophore was able to interact intimately with neighboring G bases (the most likely interaction in the case of intercalation), so effective quenching by the G bases occurred in the mismatched duplexes. In contrast, duplexes containing 4′PyT/A base pairs exhibited strong emission, since in this case the fluorophores were positioned in the minor groove and able to escape fluorescence quenching by the G bases.

Introduction

The importance of DNA sequence identification is increasing as our knowledge of the association between genotypes and phenotypes accumulates. Recently there has been growing interest in single-nucleotide polymorphisms (SNPs), due to their significant biological and clinical importance. A number of SNP-typing methods have been developed in attempts to establish an ideal typing system that would be highly sensitive, robust, and high throughput (multiplexed) without involving a costly and time-consuming step.[1] Fluorescence-labeled DNA probes have played an important role in these recent developments in the detection of single-base alterations. The single-base discrimination involved in nearly all the reported methods has been achieved, directly or indirectly, by exploiting the differences in hybridization efficiency between matched and mismatched target DNA/probe DNA duplexes.

In as far as the detection relies on hybridization events, however, such DNA probes have inherent limitations in their selectivity. Differences in hybridization efficiency vary with sequence context and are often very small for the detection of a single-base mismatch in a long target strand of DNA. To attain a high enough signal-to-noise ratio, the hybridization and washing conditions need to be carefully selected to minimize any undesirable responses from mismatched hybridization probes. From this perspective, alternative probes that do not rely on hybridization events are urgently required.[2]

Recently, "intelligent" fluorescently labeled nucleic acids probes capable of detecting single-base mismatches independently both of the state of hybridization of the probe and of enzymatic assistance have been developed.[3–6] Many such probes contain some intercalating fluorophore in place of the DNA base, positioned next to the mismatched base pair.[3] The fluorescence of the intercalator is responsive to local perturbations arising as a consequence of the presence of an adjacent mismatched base pair. Our group has recently developed base-discriminating fluorescent (BDF) oligonucleotides probes for discrimination of single-base alterations.[4,5] The concept of BDF probes is based on the fluorescence change of the BDF base itself in response to the bases on a complementary strand.[4–6] Although such BDF probes enable us to distinguish single-base alterations simply by mixing them with the target oligodeoxynucleotides (ODNs), their universal application is limited by the fluorescence quenching from the flanking bases that sometimes occurs. The fluorescence of a BDF base is considerably suppressed, especially so when the flanking base pair of the BDF probe is a G/C base pair.[4] We have recently provided a solution to this problem, by developing novel BDF probes—^{Py}U and ^{Py}C—in which a pyrenecarbonyl group is attached to uracil or cytosine at C-5 through a rigid propargyl linker.[5] ^{Py}U and ^{Py}C distinguish single-base alterations by the change in fluorescence induced by the difference in polarities between the inside and the outside of the DNA double helix. The fluorescence of the BDF nucleosides is not quenched by flanking base pairs, presumably because of the rigid propargyl linker; this prevents the fluorophore from reaching close proximity to the G sites.

[a] *Prof. Dr. I. Saito*
NEWCAT Institute, School of Engineering, Nihon University
Tamura, 963-8642 Koriyama (Japan)
Fax: (+81) 24-956-8924
E-mail: saito@mech.ce.nihon-u.ac.jp

[b] *Dr. C. Dohno*
Department of Synthetic Chemistry and Biological Chemistry
Faculty of Engineering, Kyoto University
615-8510 Kyoto (Japan)

[c] *Dr. C. Dohno, Prof. Dr. I. Saito*
SORST, Japan Science and Technology Corporation
4-1-8 Honcho, Kawaguchi, 332-0012 Saitama (Japan)

 DOI: 10.1002/cbic.200400325

For the BDF probes discussed above, G-specific quenching is recognized as being a major drawback to their general utility. If this G-specific quenching could be switched on and off through base pairing with a BDF base, however, then this quenching process could be used to advantage in single-base discrimination.

There have been many reports that neighboring nucleobases can quench the fluorescence of fluorophores.[7,8] In particular, guanine exhibits exceptionally high quenching efficiency with many different types of fluorescent labels. Since guanine is the most electron-donating of all the four bases, fluorescence quenching takes place easily through electron transfer and/or the formation of a complex with G.[7,8] In both cases, close proximity of the fluorophore and G is preferable for efficient quenching. The fluorescence can be also quenched by remote G sites by an electron-transfer mechanism through the π-stacked DNA helix when the fluorophore is efficiently stacked within the DNA double helix.[9,10] An intercalating and electron-accepting fluorophore is therefore susceptible to quenching by neighboring G sites, but can exhibit enhanced fluorescence if it is constrained so as to be positioned away from the DNA helix.

In this paper we describe a new approach to achieve the discrimination of single-nucleotide alterations through G-specific fluorescence quenching. We have developed a new BDF nucleoside, 4′-pyrenecarboxamide-modified thymidine (4′PyT), which exhibits intense fluorescence only when the 4′PyT is involved in a complementary base pair with A. Pyrenecarboxamide was selected as the fluorophore, due to its intercalative activity and its reactive quenching by G.[11] Stable base-pairing with A locates the fluorophore in the minor groove, where the fluorophore escapes efficient quenching by the flanking G bases. The pyrene group cannot intercalate within the DNA in keeping with the base pairing, due to the short methylamide linker in the 4′-position.[11g] In contrast, when the complementary base of 4′PyT is mismatched (T, G, or C), then the hydrophobic pyrenyl group is likely to intercalate with the π-stacked DNA helix, breaking the now weak hydrogen bonds. This intercalation enables the fluorophore to come into intimate contact with the flanking base pairs and results in the quenching of the fluorescence. These results confirm our concept that a single-nucleotide alteration can be distinguished through fluorescence quenching by flanking G bases. 4′PyT-containing DNA thus exhibits A-selective fluorescence, and can act as an effective probe for homogeneous SNP typing.

Results and Discussion

The synthesis of 4′PyT-containing DNA was achieved by post-modification of an ODN containing 4′-aminomethylthymidine (**2**), as outlined in Scheme 1. The phosphoramidite of 4′-aminomethylthymidine was prepared by a previously reported method[12] and was incorporated into the DNA by conventional phosphoramidite chemistry. The 4′-amino group was then converted into the desired pyrenecarboxamide group by treating it with the succinimidyl ester of pyrene-1-carboxylic acid. The sequences of the 4′PyT-containing ODNs are listed in Table 1. Fluorescence measurements were performed on each ODN hybridized with different complementary bases (N = A, C, G, or T).

Table 1. Oligodeoxynucleotide sequences used in this study.

	Sequences[a]
ODN GXT	5′-CGC AA**G X** TAA CGC
CNA (N)	3′-GCG TTC **N** ATT GCG
ODN GTXT	5′-CGC A**GT X** TAA CGC
CANA (N)	3′-GCG TCA **N** ATT GCG
ODN TXG	5′-CGC AAT **X G** AA CGC
ANC (N)	3′-GCG TTA **N** CTT GCG
ODN CXC	5′-CGC AAC **X** CAA CGC
GNG (N)	3′-GCG TT**G N G**TT GCG
GGQ	3′-**G G**TT GCG
ODN TXT	5′-CGC AAT **X** TAA CGC
ANA (N)	3′-GCG TTA **N** ATT GCG
ODN CP	5′-CCT GTG **X** TTA ATT
CCP (N)	3′-GGA CAC **N** AAT TAA

[a] X denotes 4′PyT.

We first measured the fluorescence spectra of the 4′PyT-containing ODN **GXT**, with a single G situated adjacent to 4′PyT on the 5′-side (Table 1). The ODNs were hybridized with their complementary strands: one was fully matched (N = A), and the others each contained a single mismatch (N = C, G, or T) opposite 4′PyT. The fluorescence spectra of single-stranded **GXT** and of the duplexes (N = A, C, G, or T) are shown in Figure 1. As would be expected, the fluorescence of the single-stranded **GXT** was very weak ($\Phi_F = 0.012$),[13] due to efficient quenching by the flanking G. Similar or more pronounced quenching was observed for the all the single-base mismatched duplexes. In marked contrast, the matched duplex (N = A) showed prominent fluorescence, with two emission maxima at $\lambda = 380$ and

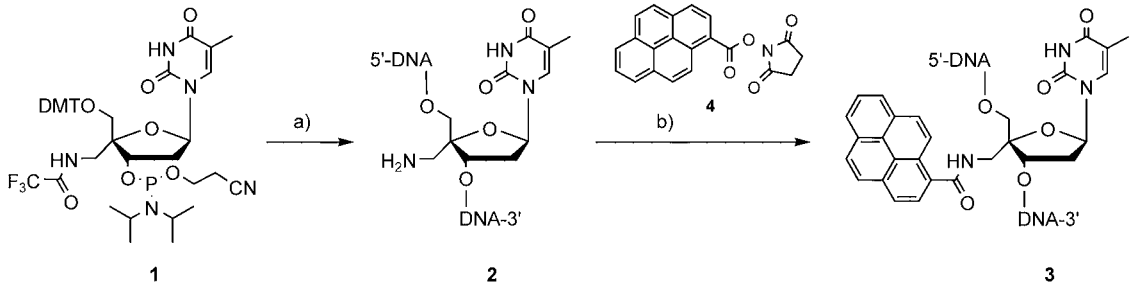

Scheme 1. Reagents and conditions: a) i) automated DNA synthesis, ii) NH_4OH, 55 °C. b) **4**, DMF, sodium phosphate buffer (pH 8.5), 37 °C.

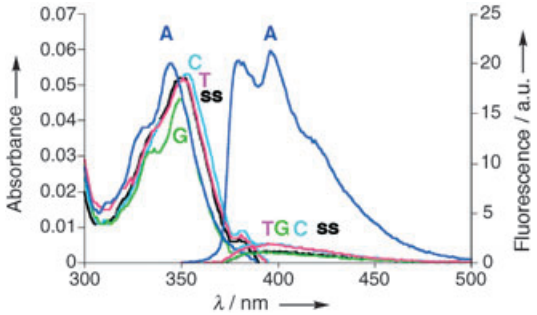

Figure 1. Absorption and fluorescence spectra of 2.5 μM **GXT** hybridized with 2.5 μM **CNA (N)** (N = A, C, G, or T; 50 mM sodium phosphate, 0.1 M sodium chloride, pH 7.0, 25 °C). "ss" denotes single-stranded **GXT**. Excitation wavelength was 345 nm.

396 nm ($\Phi_F = 0.11$) (Table 2). The fluorescent quantum yield was eight to 14 times those of the mismatched or single-stranded ODNs (Table 2). The enhanced fluorescence can be explained if we assume that the pyrenecarboxamide fluorophore was extruded from the inside of the DNA helix because of the tight base pairing of the matched 4′PyT/A. The spatial separation between the fluorophore and the flanking G precludes a quenching pathway. On the other hand, the instability of the mismatched base pairs provides more conformational freedom for approaching the flanking G. In support of this hypothesis, the absorption maxima are shifted to longer wavelengths (4–8 nm) in the absorption spectra of the mismatched duplexes (Figure 1). This red-shifted absorption suggests that the fluorophore has interacted more strongly with neighboring bases in the mismatched duplexes than in the matched duplex. An intimate interaction with G, such as intercalation of the pyrenyl group, should permit effective quenching.[14]

Table 2. *Photophysical properties of **GXT** hybridized with **CNA (N)**.*[a]

N	T_m [°C]	λ_{max} [nm]	$\varepsilon_{\lambda_{max}}$	ε_{345}[c]	λ_{em} [nm][c]	Φ_F[d]
A	50.1 (−0.8)[b]	345	22400	22400	380, 396	0.11
T	46.2 (+3.1)	351	20800	18400	396	0.014
G	43.5 (+3.5)	349	18400	14400	395	0.0077
C	47.0 (+5.0)	353	21200	18400	397	0.0081
ss		350	20800	19200	394	0.012

[a] Duplex (2.5 μM) in sodium phosphate/sodium chloride (50 mM/0.1 M, pH 7.0) at 25 °C. [b] The values in parentheses are ΔT_m between 4′PyT-containing duplexes and unmodified duplexes. [c] $\lambda_{ex} = 345$ nm. [d] The fluorescence quantum yields (Φ_F) were calculated as in ref. [13].

We next investigated the influence of the relative position of G on the 4′PyT fluorescence (Figure 2). The ODN **TXG** has a single G adjacent to 4′PyT on the 3′-side, in an otherwise identical sequence, and the fluorescence spectra of **TXG** are shown in Figure 2a. The fluorescence properties are quite similar to those of **GXT**, showing A-selective fluorescence. The polarity of DNA has an effect on the emission band shape, suggesting a different ground-state interaction, but this polarity does not have any effect on the selective fluorescence enhancement. The inset in Figure 2b shows the fluorescence spectra of the ODN **CXC** with two adjacent Gs in the complementary strand. The strongest emission seen in the inset of Figure 2b was observed for single-stranded **CXC**. In this sequence, no proximal G was present in the single-stranded state, whereas two adjacent Gs were available on hybridization with the complementary strands, so G-specific quenching is only effective after hybridization, and not for the single-stranded **CXC**. This situation was improved on by adding a short G-rich ODN **GGQ**, which functioned as a quencher for the single-stranded **CXC** (Figure 2b). The fluorescence of single-stranded **CXC** was markedly quenched by the addition of **GGQ**, while that of the duplex remained almost unchanged. Hybridization between **CXC** and the complementary strands was unaffected by the addition of the short and mismatched **GGQ**, so the addition of **GGQ** resulted in A-selective fluorescence. In contrast, the selective fluorescence was completely abolished when the neighboring Gs were removed (**TXT**, Figure 2c). G-specific quenching is an essential process for base-discriminating fluorescence,

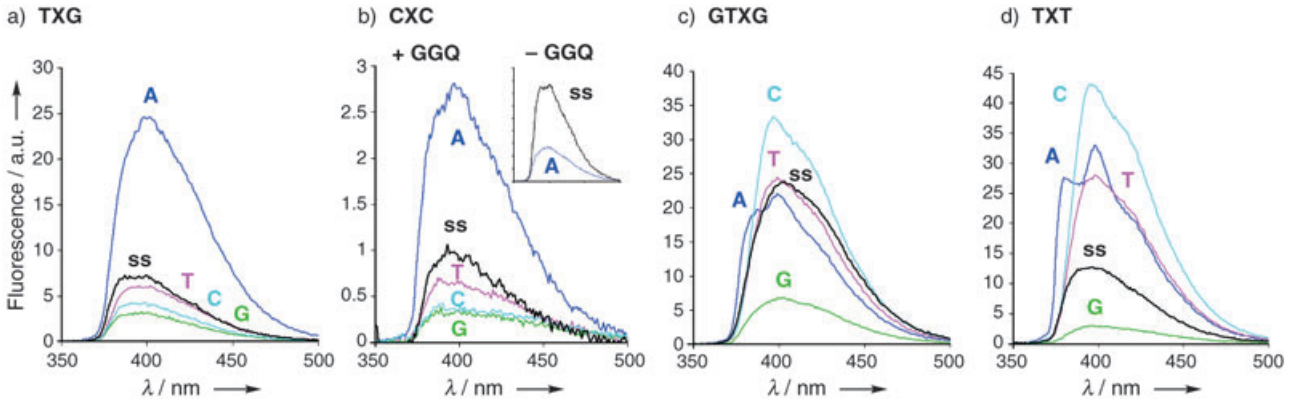

Figure 2. Influence of the location of G on the fluorescence of 4′PyT-containing ODNs. Fluorescence spectra were measured under the same conditions as in Figure 1. Spectra are shown for a) **TXG**, b) **CXC** with **GGQ** (inset: without **GGQ**), c) **GTXT**, and d) **TXT**. Excitation wavelength was 347 nm.

and the above results clearly show that 4′PyT-containing DNA exhibits A-selective fluorescence when G is positioned adjacent to 4′PyT.

All of the above tested sequences contained adjacent G sites for efficient quenching. Since DNA-mediated electron transfer enables fluorescence quenching by distant G sites,[9,10] we examined the fluorescence properties of **GTXT**, in which 4′PyT is separated from the G by an intervening thymine base. The obtained fluorescence spectra were very similar to the spectra of **TXT**, and no A-selective fluorescence was observed (Figure 2d). The similarities between **GTXT** and **TXT** indicated that quenching from neighboring guanine was no longer effective in **GTXT**.[16] Suitable quenching only occurred in sequences containing G adjacent to 4′PyT, probably due to insufficient donor–bridge–acceptor electronic coupling in this system.[9a,b]

Obvious A-selective fluorescence suggests an environmental alteration around the pyrenecarboxamide fluorophore upon base pairing with A. The fluorescence properties are highly dependent on the location of the nearest G, which determines the quenching efficiency. Therefore, the remarkable florescence of the matched duplexes would be expected to arise from increased distances and weakened interactions between 4′PyT and the G bases. We presume that the pyrenyl group was located in the minor groove in the matched duplexes, while it intercalated into the base stack in the mismatched duplexes. Figure 3 shows the optimized structures of the matched or mismatched duplexes 5′-d(CAATXTAAC)/3′-d(GTTANATTG) (N = A or T). Molecular modeling simulation was carried out by using the MacroModel v8.1 software package and the AMBER* force field. In the optimized structure of the matched duplex (N = A), the pyrenecarboxamide fluorophore was extruded from inside the DNA helix and became positioned in the minor groove. The pyrenyl group cannot intercalate into the helix in keeping with the base pairing, due to the short methylamide linker at the 4′ position. In this structure then, the fluorophore is separated from neighboring bases and so avoids the quenching pathway. In the structure of the mismatched duplex (N = T), on the other hand, the pyrenyl group intercalates deeply into the helix. The thymine base of 4′PyT is flipped out; this allows intercalation by the pyrenyl group. The fluorescence of the intercalating fluorophore, which is now brought into close proximity to the neighboring bases, is readily quenched by electron transfer from the G bases and/or by formation of ground-state complexes.[7,8] Our modeling study convincingly explains the A-selective fluorescence of 4′PyT-containing ODNs.

The proposed structures are in good agreement with our observations, such as the red-shifted absorption (Figure 1) and the increased stabilities of the mismatched duplexes (Table 2). The circular dichroism (CD) spectra of the matched and mismatched **GXT** duplexes are shown in Figure 4. The appearance of induced CD indicates that the achiral pyrenecarboxamide chromophore is situated in the chiral environment of the DNA helix. Correlation between induced CD and the type of interaction has been deduced for a variety of benzo[*a*]pyrene adduct conformations,[17] and it has been reported that groove-localized chromophores show positive induced CD bands while intercalated chromophores can show either positive or negative induced CD bands.[17,18] Interestingly, all the mismatched duplexes exhibit negative induced CD spectra, while the induced

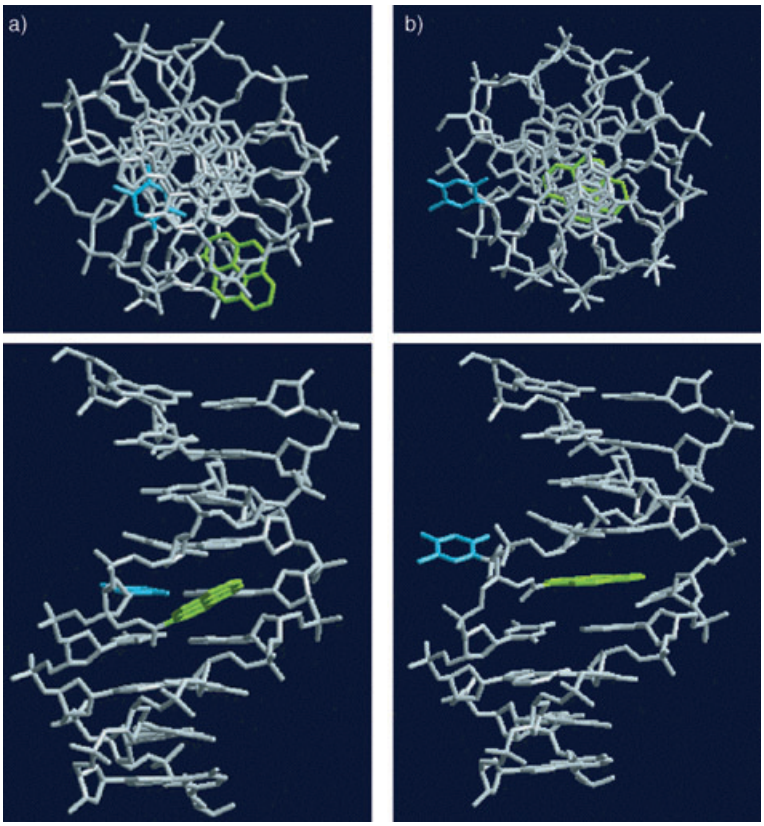

Figure 3. Molecular modeling of the conformations of the duplexes 5′-d(CAATXTAAC)-3′/5′-d(GTTANATTG)-3′ (N = A or T). The model structures were optimized by use of the AMBER* force field in water with MacroModel Version 8.1. Top views (top) and side views from the minor groove (bottom) are shown. The pyrenyl group and the thymine base of 4′PyT are represented in green and blue, respectively. a) N = A, b) N = T.

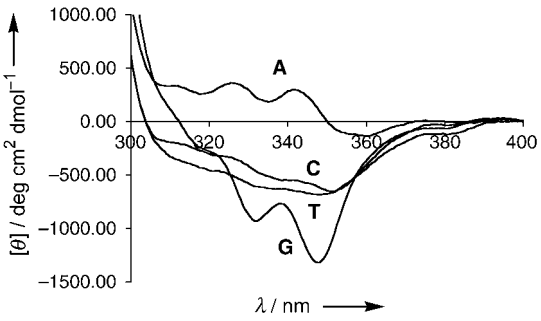

Figure 4. Induced CD spectra (300–400 nm) of 2.5 μM **GXT** hybridized with 5 μM **CNA (N)** (N = A, C, G, or T; 50 mM sodium phosphate, 0.1 M sodium chloride, pH 7.0, 25 °C). "ss" denotes single-stranded **GXT**.

CD of the matched duplex, in marked contrast, is found to be positive. The signs of our induced CD spectra fully agree with the locations of the pyrenyl groups in the calculated structures (Figure 3). In support of these results, negative induced CD bands have also been observed for benzo[*a*]pyrene adducts in mismatched duplexes as a result of base-displaced intercalation of the pyrenyl chromophore.[17]

For further confirmation of the proposed structures, we examined fluorescence quenching by potassium iodide (KI), as an external quencher. The fluorescence of a surface-exposed fluorophore is susceptible to quenching by an external quencher, so quenching provides an indication of the solvent accessibility of the fluorophore. An intercalating fluorophore can be strongly protected from collisional quenching, while a groove-localized fluorophore is more solvent-exposed.[19] Stern–Volmer plots of F_0/F versus the concentration of KI are shown in Figure 5. The ODN **TXT** was used in these experiments, because intense fluorescence unaffected by proximal Gs is observable.[20] As expected, the pyrenecarboxamide fluorophore in single-stranded **TXT** exhibits a steep gradient; this indicates that the fluorophore is highly solvent-accessible. In contrast, the fluorescence of the mismatched duplexes (N = C, T, and G) exhibited much lower quenching rates. The low gradient verifies that the fluorophores in the mismatched duplexes are not solvent-accessible, suggesting that the pyrenyl group is deeply stacked in the DNA helix. The fully matched duplex exhibits a quenching efficiency comparable to that observed for the single-stranded **TXT**. This efficient quenching can be explained by regarding the fluorophore as being positioned in the minor groove and hence more solvent-exposed than the intercalated fluorophore. Similar results were found when guanosine 5′-monophosphate was used as a quencher. The A-selective fluorescence was therefore attained by changing the environment of the pyrenecarboxamide fluorophore, which regulates the efficiency of the G-specific quenching.

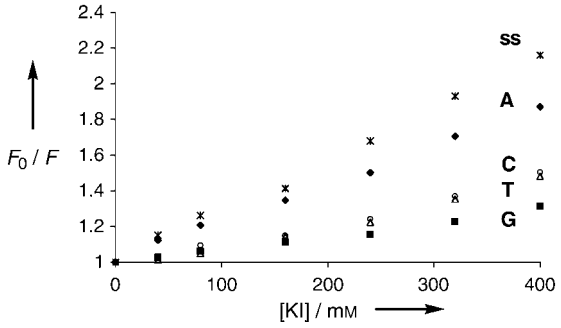

Figure 5. Stern–Volmer fluorescence quenching plots, F_0/F as a function of potassium iodide (KI) concentration. F_0 and F are the fluorescence intensities in the absence and presence of KI, respectively. Fluorescence intensities of 2.5 μM **TXT**/**ANA** (N = A, C, G, or T) were measured in the presence of varying concentrations of KI. "ss" denotes single-stranded **TXT**. Excitation wavelength was 345 nm.

This highly A-selective fluorescence is readily applicable to SNP typing. We conducted a preliminary experiment with a short 13-mer ODN **CCP** containing a wild-type (N = G) or mutant (N = A) ceruloplasmin gene sequence associated with systemic hemosiderosis in humans (Table 1).[21] The 4′PyT-containing ODN probe **CP** has a G, needed for the fluorescence quenching, adjacent to the single-base alteration site. The probe and the target ODNs were loaded on a UV-transparent quartz microplate, and their fluorescence was analyzed over the 290–365 nm range by use of a VersaDoc 3000 Imaging System fitted with a 380 nm long-pass emission filter. Figure 6 shows that the difference in fluorescence intensities was unambiguous, with the probe ODN exhibiting an intense fluorescence only when the probe was hybridized with **CCP** (A). In marked contrast, negligible fluorescence was observed for the duplex with **CCP** (G) and for the single-stranded probe. The 4′PyT-containing ODN can thus clearly discriminate a single-base alteration in the ceruloplasmin gene sequence. Since this method does not require stringent hybridization and washing conditions, the 4′PyT-containing ODN should offer advantages over conventional DNA chip techniques.

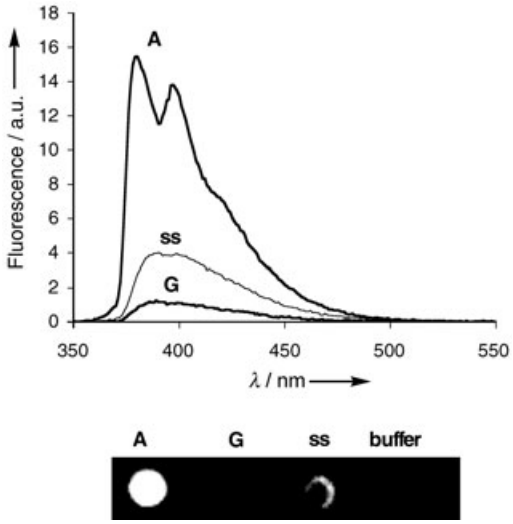

Figure 6. Discrimination of the single-base alteration in the sequence of the ceruloplasmin (Cp) gene associated with systemic hemosiderosis in humans. Target 13-mer ODNs (2.5 μM) containing wild-type (G) or mutant (A) Cp gene were mixed with 2.5 μM BDF probe (**CP**) in sodium phosphate (pH 7.0, 50 mM) and NaCl (0.1 M). Fluorescence spectra (top) and images (bottom) are shown. For fluorescence imaging, the solutions were pipetted into a 96-well quartz microplate, and illuminated with a UV transilluminator (290–365 nm). The image was taken through a 380 nm long-pass emission filter with the aid of a CCD camera. "ss" denotes single-stranded CP.

Conclusion

Interactions between a pyrenecarboxamide fluorophore and DNA changed markedly as a response to the base pairing of 4′PyT with a complementary base. In the mismatched duplexes the pyrenyl group intercalates within the DNA helix, while in the matched duplexes it is located in the minor groove. These properties are readily applicable to BDF DNA probes, employing fluorescence quenching by neighboring G sites as a base-discrimination step. Fluorescence of mismatched duplexes is

efficiently quenched due to the close proximity of Gs. In contrast, matched duplexes exhibit prominent emission, since the fluorophore is now situated away from the quenching G groups. A neighboring G/C base pair is required in the target sequence for the A-selective fluorescence of 4′PyT. Further exploration of fluorophores that are adequately quenched by remote Gs[9,10] should expand the available sequences for universally applicable BDF probes. Since gene density tends to increase in the GC-rich region,[22] DNA probes based on guanine-specific fluorescence quenching should be a powerful tool for single-base discrimination.

Experimental Section

General: The reagents for DNA synthesis were purchased from Glen Research. Molecular masses of oligodeoxynucleotides were determined with a MALDI-TOF MS (Perseptive Voyager Elite, acceleration voltage 21 kV, negative mode) with 2′,3′,4′-trihydroxyacetophenone as a matrix and with T_8 ($[M-H]^- = 2370.61$) and T_{17} ($[M-H]^- = 5108.37$) as internal standards. All aqueous solutions utilized purified water (Millipore, Milli-Q sp UF). Reversed-phase HPLC was performed on CHEMCOBOND 5-ODS-H columns (10×150 mm, 4.6×150 mm) with a Gilson Chromatograph (Model 305) and a UV detector (Model 118) at 254 nm.

Oligodeoxynucleotide (ODN) synthesis and characterization: The synthesis of 4′PyT-containing ODNs was accomplished by post-synthesis modification of 4′-aminomethylthymidine-containing ODNs. The phosphoramidite of 4′-aminomethylthymidine was prepared by the previously reported procedure.[12] ODNs were synthesized by conventional phosphoramidite methodology with an Applied Biosystems 392 DNA/RNA synthesizer. The 4′-aminomethylthymidine-containing ODN in sodium phosphate buffer (pH 8.5) was added to a DMF solution of the succinimidyl ester of pyrenecarboxylic acid (10 mM), and the system was incubated at 37 °C for 15 h. The resulting suspended mixture was filtered and evaporated to dryness.

The ODNs were purified by reversed-phase HPLC on a CHEMCOBOND 5-ODS-H column (10×150 mm) with elution with 3–15.5–36% (0–25–40 min) acetonitrile in aqueous triethylamine acetate (TEAA, 0.1 M, pH 7.0) at a flow rate of 3.0 mL min^{-1}. The concentration of the 4′PyT-containing ODN solution was determined by the absorbance at 260 nm (with 14400 M^{-1} cm^{-1} taken for 4′PyT). All ODNs were confirmed by MALDI-TOF mass spectrometry and were all within 2 mass units of the calculated values.

GXT (5′-d(CGC AAG X TAA CGC)-3′): $[M-H]^-$ calcd: 4199.9; found 4201.0.

GTXT (5′-d(CGC AGT X TAA CGC)-3′): $[M-H]^-$ calcd: 4190.9; found 4192.4.

TXG (5′-d(CGC AAT X GAA CGC)-3′): $[M-H]^-$ calcd: 4199.9; found 4201.4.

CXC (5′-d(CGC AAC X CAA CGC)-3′): $[M-H]^-$ calcd: 4144.9; found 4145.1.

TXT (5′-d(CGC AAT X TAA CGC)-3′): $[M-H]^-$ calcd: 4175.1; found 4175.9.

CP (5′-d(CCT GTG X TTA ATT)-3′: $[M-H]^-$ calcd: 4186.9; found 4187.6.

Melting temperature (T_m) measurements: All T_ms of the ODNs (2.5 μM final duplex concentration) were taken in sodium phosphate buffers (50 mM, pH 7.0) containing sodium chloride (100 mM). Absorbance/temperature profiles were measured at 260 nm with a Shimadzu UV-2550 spectrophotometer fitted with a Peltier temperature controller in a 1 cm pathlength cell. The absorbance of the samples was monitored at 260 nm from 5 °C to 90 °C with a heating rate of 1 °C min^{-1}. From these profiles, first derivatives were calculated to determine T_m values.

UV/visible absorption and CD measurements: The ODN solutions were prepared as described in the T_m measurement experiment. Absorption spectra were obtained with an Ultraspec 3000pro UV/Vis spectrophotometer (Amersham Pharmacia Biotech) at room temperature in a 1 cm pathlength cell. CD measurements were performed on a JASCO J-805 Spectropolarimeter. CD spectra were recorded over the 210–400 nm wavelength range in a cylindrical cell with a pathlength of 1 cm (165-QS). The observed rotation degrees were converted into molar ellipticity as calculated from the nucleotide concentrations.

Fluorescence experiments: The ODN solutions were prepared as described in the T_m measurement experiment. Fluorescence spectra were obtained with a Shimadzu RF-5300PC spectrofluorophotometer at 25 °C in a 1 cm pathlength cell. The excitation bandwidth was 1.5 nm and the emission bandwidth was also 1.5 nm.

Fluorescence quantum yields: The fluorescence quantum yields (Φ_F) were determined by use of 9,10-diphenylanthracene as a reference with a known Φ_F of 0.95 in ethanol.[13] The area of the emission spectrum was integrated by use of the software available for the instrument, and the quantum yield was calculated according to the following equation:

$$\frac{\Phi_{F(S)}}{\Phi_{F(R)}} = \frac{A_{(S)}}{A_{(R)}} \times \frac{(Abs)_{(R)}}{(Abs)_{(S)}} \times \frac{{n_{(S)}}^2}{{n_{(R)}}^2} \quad (1)$$

Here, $\Phi_{F(S)}$ and $\Phi_{F(R)}$ are the fluorescence quantum yields of the sample and the reference, respectively, $A_{(S)}$ and $A_{(R)}$ are the areas under the fluorescence spectra of the sample and of the reference, respectively, $(Abs)_{(S)}$ and $(Abs)_{(R)}$ are the respective optical densities of the sample and the reference solution at the wavelength of excitation, and $n_{(S)}$ and $n_{(R)}$ are the values of refractive index for the respective solvents used for the sample (1.333) and the reference (1.383).

KI titration experiments: In the KI titration experiments, small aliquots of concentrated potassium iodide (KI, 8 M) were added to the ODN solution (2.5 μM) in sodium phosphate buffer (50 mM, pH 7.0) containing sodium chloride (100 mM). Appropriate amounts of the ODN and buffer solution were also added to maintain the ODN concentrations at constant values at the different KI concentrations. Samples were mixed by pipetting up and down and were allowed to equilibrate with KI for 5 min before acquisition of spectra. The KI Stern–Volmer fluorescence quenching plots were obtained by plotting F_0/F as a function of the KI concentration, where F_0 and F are the fluorescence intensities in the absence and in the presence of KI, respectively.

Fluorescence imaging: Fluorescence imaging was performed with a Bio-Rad VersaDoc 3000. The sample solutions were pipetted into a 96-well UV transparent quartz microplate and were illuminated with a 290–365 nm transilluminator. Images were taken through a 380 nm long-pass emission filter.

Keywords: base flipping · bioorganic chemistry · guanine · intercalation · mismatches · pyrene

[1] a) P. Y. Kwok, *Annu. Rev. Genomics Hum. Genet.* **2001**, *2*, 235 – 258; b) C. S. Carlson, T. L. Newman, D. A. Nickerson, *Curr. Opin. Chem. Biol.* **2001**, *5*, 78 – 85; c) M. Chicurel, *Nature* **2001**, *412*, 580 – 582.

[2] a) S. Sauer, D. Lechner, K. Berlin, H. Lehrach, J.-L. Escary, N. Fox, G. Gut, *Nucleic Acids Res.* **2000**, *28*, e13; b) E. M. Boon, D. M. Ceres, T. G. Drummond, M. G. Hill, J. K. Barton, *Nat. Biotechnol.* **2000**, *18*, 1096 – 1100; c) K. Nakatani, S. Sando, I. Saito, *Nat. Biotechnol.* **2001**, *19*, 51 – 55.

[3] a) A. Yamane, *Nucleic Acids Res.* **2002**, *30*, e97; b) B. Christense, E. B. Pedersen, *Helv. Chim. Acta* **2003**, *86*, 2090 – 2097; c) O. Köhler, O. Seitz, *Chem. Commun.* **2003**, 2938 – 2939.

[4] a) A. Okamoto, K. Tainaka, I. Saito, *J. Am. Chem. Soc.* **2003**, *125*, 4972 – 4973; b) A. Okamoto, K. Tainaka, I. Saito, *Chem. Lett.* **2003**, *32*, 684 – 685; c) A. Okamoto, K. Tanaka, T. Fukuta, I. Saito, *J. Am. Chem. Soc.* **2003**, *125*, 9296 – 9297; d) A. Okamoto, K. Tainaka, I. Saito, *Tetrahedron Lett.* **2003**, *44*, 6871 – 6874; e) A. Okamoto, K. Tanaka, T. Fukuta, I. Saito, *ChemBioChem* **2004**, *5*, 958 – 963.

[5] A. Okamoto, K. Kanatani, I. Saito, *J. Am. Chem. Soc.* **2004**, *126*, 4820 – 4827.

[6] a) G. T. Hwang, Y. J. Seo, B. H. Kim, *J. Am. Chem. Soc.* **2004**, *126*, 6528 – 6529; b) G. T. Hwang, Y. J. Seo, S. J. Kim, B. H. Kim, *Tetrahedron Lett.* **2004**, *45*, 3543 – 3546.

[7] a) C. A. M. Seidel, A. Schulz, M. H. M. Dauer, *J. Phys. Chem.* **1996**, *100*, 5541 – 5553; b) S. A. E. Marras, F. R. Kramer, S. Tyagi, *Nucleic Acids Res.* **2002**, *30*, e122.

[8] a) M. Manoharan, K. L. Tivel, M. Zhao, K. Nafisi, T. L. Netzel, *J. Phys. Chem.* **1995**, *99*, 17461 – 17472; b) C. Knapp, J.-P. Lecomte, A. K.-D. Mesmaeker, G. Orellana, *J. Photochem. Photobiol. B* **1996**, *36*, 67 – 76; c) S. L. Driscoll, M. E. Hawkins, F. M. Balis, W. Pfleiderer, W. R. Laws, *Biophys. J.* **1997**, *73*, 3277 – 3286; d) J. M. Jean, K. B. Hall, *Proc. Natl. Acad. Sci. USA* **2001**, *98*, 37 – 41; e) K. Kawai, A. Yokoohji, S. Tojo, T. Majima, *Chem. Commun.* **2003**, 2840 – 2841.

[9] a) S. O. Kelley, J. K. Barton, *Science* **1999**, *283*, 375 – 381; b) S. Hess, M. Götz, W. B. Davis, M. E. Michel-Beyerle, *J. Am. Chem. Soc.* **2001**, *123*, 10046 – 10055; c) M. A. O'Neill, C. Dohno, J. K. Barton, *J. Am. Chem. Soc.* **2003**, *125*, 16198 – 16199; d) T. Kimura, K. Kawai, T. Majima, *Chem. Commun.* **2004**, 268 – 269.

[10] a) C. J. Murphy, M. R. Arkin, Y. Jenkins, N. D. Ghatlia, S. H. Bossmann, N. J. Turro, J. K. Barton, *Science* **1993**, *262*, 1025 – 1029; b) S. O. Kelley, R. E. Holmlin, E. D. A. Stemp, J. K. Barton, *J. Am. Chem. Soc.* **1997**, *119*, 9861 – 9870; c) S. O. Kelley, J. K. Barton, *Chem. Biol.* **1998**, *5*, 413 – 425; d) F. D. Lewis, R. L. Letsinger, M. R. Wasielewski, *Acc. Chem. Res.* **2001**, *34*, 159 – 170.

[11] For fluorescence properties of the pyrene-labeled DNA, see examples: a) J. S. Mann, Y. Shibata, T. Meehan, *Bioconjugate Chem.* **1992**, *3*, 554 – 558; b) V. A. Korshun, I. A. Prokhorenko, S. V. Gontarev, M. V. Skorobogatyi, K. V. Balakin, E. V. Manasova, A. D. Malakhov, Y. A. Berlin, *Nucleosides Nucleotides* **1997**, *16*, 1461 – 1464; c) F. D. Lewis, Y. Zhang, R. L. Letsinger, *J. Am. Chem. Soc.* **1997**, *119*, 5451 – 5452; d) P. L. Paris, J. M. Langenhan, E. T. Kool, *Nucleic Acids Res.* **1998**, *26*, 3789 – 3793; e) K. Yamana, H. Zako, K. Azuma, R. Iwase, H. Nakano, A. Murakami, *Angew. Chem. Int. Ed.* **2001**, *40*, 1104 – 1106; f) E. Mayer, L. Valis, C. Wagner, M. Rist, N. Amann, H.-A. Wagenknecht, *ChemBioChem* **2004**, *5*, 865 – 868; g) T. Bryld, T. Højland, J. Wengel, *Chem. Commun.* **2004**, 1064 – 1065.

[12] G. Wang, W. E. Seifert, *Tetrahedron Lett.* **1996**, *37*, 6515 – 6518.

[13] J. V. Morris, M. A. Mahaney, J. R. Huber, *J. Phys. Chem.* **1976**, *80*, 969 – 974.

[14] The energetics of electron transfer from G was estimated by use of the Rehm–Weller equation.[15] The measured singlet energy (2.92 eV) and reduction potential (−2.04 V vs. Ag/Ag^+, in DMF) of pyrenecarboxamide give the Gibbs free energy for the G oxidation as −0.21 eV.

[15] a) D. Rehm, A. Weller, *Isr. J. Chem.* **1970**, *8*, 259 – 271; b) F. D. Lewis, R. S. Kalgutkar, Y. Wu, X. Liu, J. Liu, R. T. Hayes, S. E. Miller, M. R. Wasielewski, *J. Am. Chem. Soc.* **2000**, *122*, 12346 – 12351.

[16] Since the pyrenecarboxamide fluorophore is sensitive to the polarity of its surroundings, the fluorescence properties of **GTXT** were determined predominantly by the local environment of the fluorophore.[5] The characteristic emission band shape of the matched duplex (N = A) suggested that the fluorophore was placed in a different environment than in the other, mismatched, duplexes.

[17] P. Pradhan, B. Jernström, A. Seidel, B. Nordén, A. Gräslund, *Biochemistry* **1998**, *37*, 4664 – 4673.

[18] a) P. E. Schipper, B. Nordén, F. Tjerneld, *Chem. Phys. Lett.* **1980**, *70*, 17 – 21; b) M. Kubista, B. Åkerman, B. Nordén, *J. Phys. Chem.* **1988**, *92*, 2352 – 2356.

[19] a) W. Huang, S. Amin, N. E. Geacintov, *Chem. Res. Toxicol.* **2002**, *15*, 118 – 126; b) P. Rai, T. D. Cole, E. Thompson, D. P. Millar, S. Linn, *Nucleic Acids Res.* **2003**, *31*, 2323 – 2332.

[20] The induced CD spectra of ODN **TXT** were very similar to that of ODN **GXT** (Figure 4). The pyrenecarboxamide fluorophores in the two ODN duplexes are probably situated in similar environments.

[21] K. Yoshida, K. Furihata, S. Takeda, A. Nakamura, K. Yamamoto, H. Morita, S. Hiyamuta, S. Ikeda, N. Shimizu, N. Yanagisawa, *Nat. Genet.* **1995**, *9*, 267 – 272.

[22] International Human Genome Sequencing Consortium, *Nature* **2001**, *409*, 860 – 921.

Received: September 10, 2004
Published online on April 25, 2005

